Available online at www.sciencedirect.com

ScienceDirect

www.elsevier.com/locate/jes

JES JOURNAL OF ENVIRONMENTAL SCIENCES

www.jesc.ac.cn

Assessment of column aerosol optical properties using ground-based sun-photometer at urban Harbin, Northeast China

Qixiang Chen[1], *Yuan Yuan*[1,*], *Xing Huang*[2], *Zhihong He*[1], *Heping Tan*[1]

1. *Key Laboratory of Aerospace Thermophysics, Ministry of Industry and Information Technology, Harbin Institute of Technology, 92 West Dazhi Street, Harbin 150001, China*
2. *College of Metallurgy and Energy, North China University of Science and Technology, 21 Bohai Street, Tangshan 063009, China*

ARTICLE INFO

Article history:
Received 17 September 2017
Revised 24 January 2018
Accepted 6 February 2018
Available online 19 February 2018

Keywords:
Sun-photometer
Column aerosol property
Aerosol type
Urban Harbin
Northeast China

ABSTRACT

Aerosol plays a key role in determining radiative balance, regional climate and human health. Severe air pollution over Northeast China in recent years urges more comprehensive studies to figure out the adverse effects caused by excessive aerosols. In this study, column aerosol measurements over urban Harbin, a metropolis located at the highest latitude in Northeast China, during May 2016 to March 2017 were conducted using a CIMEL sun-photometer to analyze local aerosol properties and its variation from different aspects. According to the observations, aerosol optical depth at 440 nm (AOD_{440}) ranges from 0.07 up to 1.54, and the large variability in both AOD_{440} and Angstrom Exponent ($AE_{440-870}$) indicates the frequent change of aerosol types due of different emission sources. Coarse mode particles dominated Harbin during the studying period because of the long-range transported dust and probably the suspended snow crystals in winter. As the wavelength increases, relatively consistent decrease trends of single scattering albedo (SSA) and asymmetry factor (ASY) were observed in spring, autumn, and winter, indicating the presence of absorbing polluted aerosols. Mixed type (MIX) aerosol dominated the study region with a total percentage of 34%, and biomass burning and urban industry (BB/UI), clean continental (CC), and desert dust (DD) aerosols were found to be 31%, 27%, and 8%, respectively. The current work fills up the optical characteristics of aerosols in Harbin, and will contribute to the in-depth understanding of local aerosol variation and regional climate change over Northeast China.

Introduction

Aerosol is one of the most important constituents of atmosphere. It contributes significantly to climate change due to its influence on atmospheric chemical reactions and impact on cloud formation, earth radiation budget, and plant growth rate (Dubovik et al., 2000; Tanre et al., 2001). Episodic studies show that overexposure to high concentration of polluted aerosols will lead to forced-breathing and increased mortality (Bai et al., 2016; Jiang et al., 2017; Zou et al., 2017). Different from trace greenhouse gases, it is more difficult to investigate the environmental effect of aerosol due to multiple reasons (Shi, 2007). Aerosol consists of various substances with different size distributions, particle shapes, and chemical compositions, and thus has different optical properties, which may cause contrary climate effects (Haywood et al., 2003; Takemura et al., 2002).

* *Corresponding author. E-mail:* yuanyuan83@hit.edu.cn (Yuan Yuan).

https://doi.org/10.1016/j.jes.2018.02.003
1001-0742/

Aerosol particles are emitted by abundant sources and have a transient life period, which adds the complexities and uncertainties in aerosol studies (Mao, 2016; Smirnov et al., 2003; Wang et al., 2017). Therefore, large scale and high temporal resolution measurements of aerosol are necessary to understand their environmental impact. Ground-based sun-photometer is a fundamental measurement characterizing aerosol microphysical and optical properties at high quality levels due to its wide angular and spectral measurements of solar and sky radiation (Garcia et al., 2012; Russell et al., 2004; Xia et al., 2016). The observations are widely used to characterize local aerosol optical properties, to evaluate satellite aerosol products, and to understand aerosol-cloud-radiation interactions (Xia et al., 2016, 2007).

Many studies on aerosol optical properties have been made in North China Plain, Yangtze Delta region and western regions (Xia et al., 2007, 2013). However, compared with the mentioned regions above, more attention should be paid to Northeast China region, the heavy industry base of China. Extensive industrialization and half-year-long heating period expose the cities to intense hazes events, especially in winter (Yu et al., 2016; Zhang et al., 2016). And PM2.5 concentrations exceed limits frequently (Chen et al., 2017; Kuang et al., 2016). Hence, there is an urge demand that continuous measurement should be implemented in this heavily polluted region to assess aerosol impact on regional environment and climate over Northeast China (Li et al., 2015; Zhu et al., 2014). Although aerosol optical properties over Northeast China have been studied by previous researchers, little focus has been paid to Harbin, the northern-most metropolis. This work attempts to perform a comprehensive study of local aerosol properties at Harbin. And to the best of our knowledge, it is the first time that both aerosol optical and microphysical properties at Harbin has been studied.

In this study, data from nine-month observation at urban Harbin were used to analyze local aerosol microphysical and optical properties, as well as the variation of aerosol types. In the section "Materials and methods," a brief description of the regional characteristics, instruments, data analysis methods, and related dataset is given. In the "Results and discussion" section, we describe a comprehensive analysis of local aerosol properties, such as aerosol optical depth (AOD), angstrom exponent (AE), water vapor (WV), volume size distribution (VSD), single scattering albedo (SSA), and asymmetry factor (ASY), together with aerosol type changes. Also, a case study of urban haze was analyzed using space-borne Lidar measurement and the HYSPLIT back trajectory method. At last, we present a concise conclusion.

1. Materials and methods

1.1. Site description

Harbin (125.4°E–130.1°E, 44.0°N–46.4°N) has a total urban area of 10,200 km^2 and a population of 5.5 million. It is located at the highest inhabited latitude and records the lowest temperature as a provincial capital and metropolis in China (Fig. 1). Harbin is subject to continental monsoon climate. Summer (July–August) is characterized by hot, damp and rainy weather while winter (October–March) is cold, and dry.

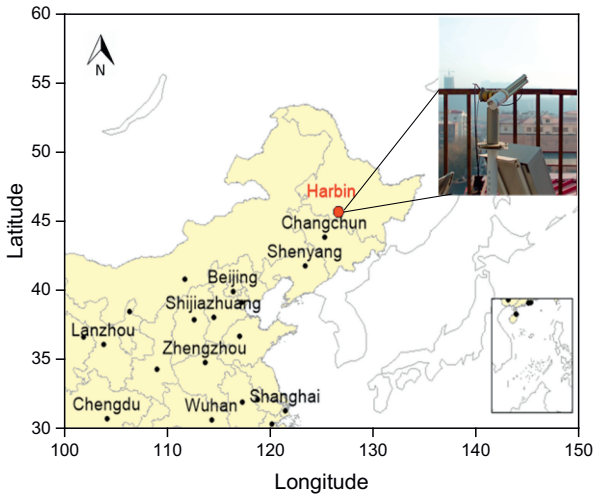

Fig. 1 – The geographical position of the studying area, and the CE-318 sun-photometer.

Local meteorological parameters such as rainfall, temperature, relative humidity, and wind speed were obtained from the China Meteorological Administration. The distribution of monthly mean total rainfall is shown in Fig. 2a. The distribution shows that precipitation mainly concentrated during May–October, with a peak of 150 mm in June, while snow falls in November to March with negligible rainfall. The total rainfall during May 2016 to March 2017 is 397.5 mm, which is much less than those over south China region. The monthly mean of ambient temperature and relative humidity (RH) is plotted in Fig. 2b and c. The temperature reaches nearly 30 °C in summer (July–August), thereafter gradually decreases towards January, with the lowest temperature at −20 °C, and then it goes up by degrees from February. A bi-model distribution of RH is observed, with two-peak value around 90% in July and December, while RH values in May and October are relatively low with an average monthly RH less than 60%. Monthly variation of wind speed is illustrated in Fig. 2d, and the change is relative small, where a maximum monthly wind speed is observed (17 m/s) in May. The present study focuses on three seasons: spring (May–June), autumn (September–October) and winter (November–March).

1.2. Measurement

The instrument used in this study is a CE318 sun-photometer (CIMEL, France). The automatic sun-photometer provides two kinds of basic measurements: direct sun and diffuse sky radiance observations. There are eight spectral bands inside the sensors, with 1.2° full field of view, between 0.34 and 1.64 μm. More details of the instrument can be found in several earlier works (Dubovik et al., 2000, 2002; Smirnov et al., 2003). AOD, AE, and WV were three main outputs of the sun-photometer, which could be accurately calculated. Particle size distribution and refractive index are retrieved using eight spectral AODs, then aerosol optical properties like SSA and ASY are calculated based on the above parameters. Detailed inversion scheme is presented in Appendix part.

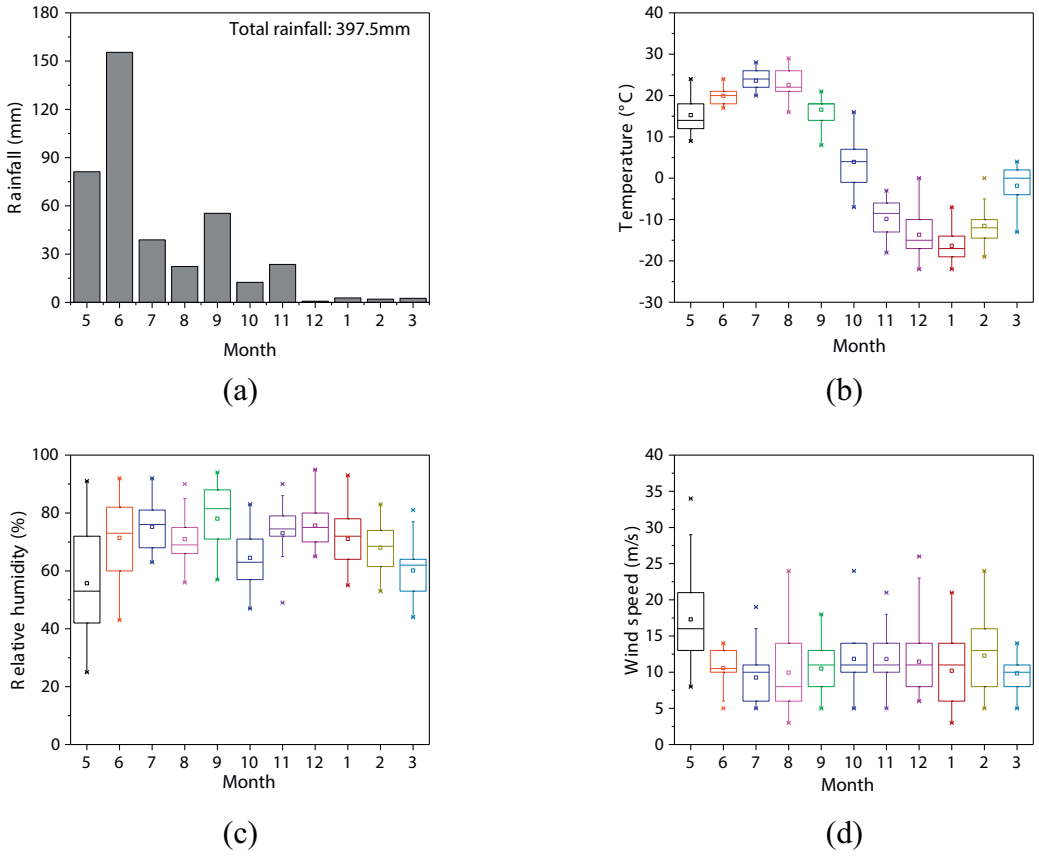

Fig. 2 – The climatological distribution of (a) total rainfall, (b) air temperature (in °C), (c) relative humidity (in %), and (d) wind speed (in m/sec) describes as box plots during the period from May 2016 to March 2017 over urban Harbin. In each box, the central line is the median and the lower and upper limits are the first and the third quartiles, respectively. The lines extending vertically from the box indicate the spread of the distribution with the length being 1.5 times the difference between the first and the third quartiles. The asterisk symbols indicate the geometric means.

2. Results and discussion

2.1. *Temporal variation of local aerosols*

AOD is corresponding to the atmospheric column aerosol load, while AE is representative of the aerosol size. The temporal variation of daily mean AOD_{440}, $AE_{440–870}$, and WV is presented in Fig. 3. On the overall scale, local AOD_{440} ranges from 0.07 up to 1.54. Low AOD_{440} (<0.1) is regarded as clean background air conditions, while high AOD_{440} (>0.5, or even >1.0) represents the severe aerosol burden in the atmosphere due to the influence of transport dust or anthropogenic pollutants (Xin et al., 2007). The large daily variability in both AOD_{440} and $AE_{440–870}$ indicates the frequent change of aerosol types over urban Harbin because of different emission sources. The seasonal statistics of AOD_{440}, $AE_{440–870}$ and WV (in cm) over urban Harbin during the study period are presented in Table 1. Daily mean AOD_{440} at Harbin is 0.42 ± 0.29, which is familiar with the annual mean AOD_{440} 0.42 ± 0.32 at Kunming (Zhu et al., 2016) and 0.44 ± 0.30 at Urumqi (Li et al., 2017). And the annual mean AOD is lower than many urban areas of China, like the Yangtze Delta region, the North China Plain and central China (Li et al., 2007; Xia et al., 2016, 2007).

Seasonal mean AOD_{440}, $AE_{440–870}$, and WV (in cm) during spring are respectively 0.40 ± 0.27, 1.41 ± 0.38, and 1.64 ± 0.46 cm, while they are respectively 0.43 ± 0.26, 1.85 ± 0.96, and 1.07 ± 0.19 cm during autumn and 0.42 ± 0.32, 1.13 ± 0.28,

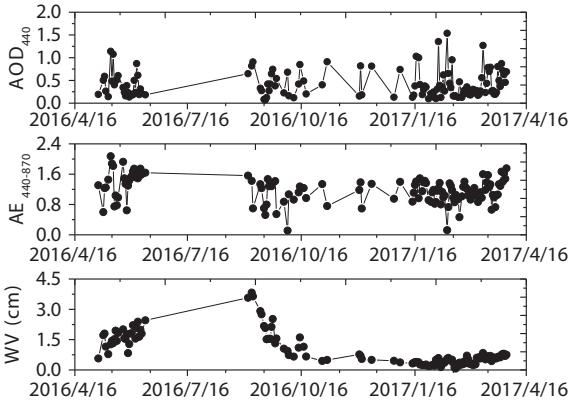

Fig. 3 – Daily variation of (a) aerosol optical depth at 440 nm, (b) Ångström exponent at 440–870 nm, and (c) columnar water vapor (in cm) over urban Harbin during the study period.

Table 1 – Seasonal variability of AOD_{440}, $AE_{440–870}$ and WV (in cm) over urban Harbin during the studying period.

Season	AOD_{440}	$AE_{440–870}$	WV(cm)
Spring(May-Jun)	0.40 ± 0.27	1.41 ± 0.38	1.64 ± 0.46
Autumn(Sep-Oct)	0.43 ± 0.26	1.85 ± 0.96	1.07 ± 0.37
Winter(Nov-Feb)	0.42 ± 0.32	1.13 ± 0.28	0.46 ± 0.19
Total	0.42 ± 0.29	1.18 ± 0.34	0.97 ± 0.79

AOD_{440}: aerosol optical depth at 440 nm; $AE_{440–870}$: angstrom exponent between 440 nm and 870 nm; WV: water vapor (in cm).

and 0.46 ± 0.19 during winter. During spring (May–June), seasonal mean AOD_{440} is the lowest with the highest WV and moderate $AE_{440–870}$, indicating that the particle size is larger than that in autumn, and it is likely related to the mixing of transported dust from west and anthropogenic pollutants (Zhu et al., 2014, 2016). Highest AOD_{440} as well as $AE_{440–870}$ is observed in autumn and implies that aerosols during this period is characterized by fine mode particles, which is due to the transported aerosol loads from the south, local industrial emission and automobile exhaust, which is similar to other metropolis in China (Yu et al., 2009b; Zhang and Mao, 2015). Winter is more prone to static weather, and the frequency of severe pollution is much higher than other seasons (Wang et al., 2016). $AE_{440–870}$ values are stable near 1.2 in winter, which means the dominance of fine mode particles over this region (Xia et al., 2016). Similar to North China Plain, winter at Harbin is even more cold and dry, which does not favor for the aerosol hygroscopic growth. Lowest seasonal mean $AE_{440–870}$ is observed in winter because of relative high wind speed (Fig. 2d), and it would result in the mixing state of transported dust and local anthropogenic emissions.

2.2. Volume size distribution (VSD)

Columnar aerosol size distribution is a key parameter determining the aerosol optical properties, which is closely related to AE and its variations (Yu et al., 2009b). In general, the fine mode particles are mainly related to anthropogenic activities, such as fuel combustion and vehicle exhaust, while the coarse mode particles are inclined to be composed of local suspended dust by strong wind or emitted from building construction and long range transported dust from desert (Cheng et al., 2015).

Fig. 4 shows the seasonal mean of aerosol volume size distribution over urban Harbin. The aerosol volume size distributions are found to be bimodal logarithm normal structure with the fine mode radius <0.6 μm and coarse mode radius >0.6 μm. The volume concentration of fine mode particle reaches peak at radius 0.19 μm during spring and winter, and at radius 0.25 μm during autumn. The coarse mode showed the maxima peak at radius 2.9 μm, 5.1 μm, and 4.0–8.0 μm during spring, autumn, and winter respectively. The increase of both fine and coarse mode radius during autumn may be attributed to the hygroscopic growth of particles because of the relatively high rainfall and high RH condition during the late monsoon season (September and October). The coarse mode particles are obviously dominant over urban Harbin during spring, and this is mostly due to the presence of transport dust particles, where a

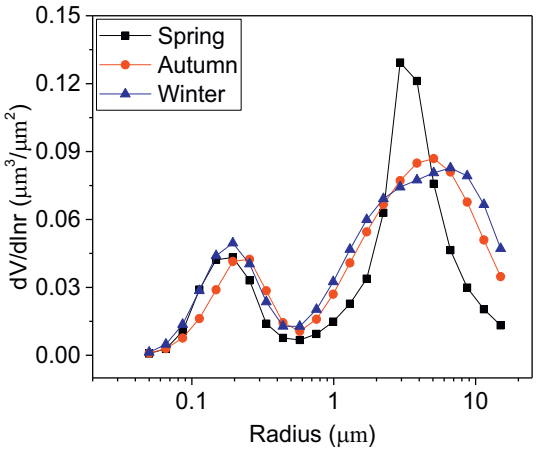

Fig. 4 – Seasonal variation of volume size distribution over urban Harbin during May 2016 to March 2017.

familiar seasonal mean volume size distribution during spring is observed in SACOL and Beijing site (Che et al., 2014; Li and Zhang, 2012; Yu et al., 2016). Due to its geographical environment characterized of flat terrain and prevailing wind and sand, which is familiar to the west site, SACOL (Che et al., 2014; Li and Zhang, 2012; Yu et al., 2016), Harbin has often been affected by the transported dust during the studying period. The coarse mode particles also dominate during winter and shows a higher coarse mode radius, which indicates the long range transported dust aerosols and probably the presence of suspended snow crystals, and this increase could also be found in winter SACOL (Che et al., 2014; Li and Zhang, 2012). The volume concentration of fine modes is slightly larger during winter compared to other seasons, suggesting the abundance of anthropogenic emissions like soot particles due to heating and the existence of coagulation of aerosols under the often occurring weather conditions which are harmful to the diffusion of pollutants (Patel et al., 2017).

2.3. Single scattering albedo (SSA)

SSA is defined as the ratio of scattering to total extinction of solar radiation and is one of the most important aerosol properties in acquiring the absorption and scattering characteristics of suspended particles (Patel et al., 2017). Weakly absorbing particles, like sulfate, has high SSA_{440} values (>0.95), while strongly absorbing aerosols, like soot or black carbon, has low values (<0.85). SSA for moderately absorbing and slightly absorbing aerosols is in the range of 0.85–0.90 and 0.90–0.95, respectively. Additionally, the spectral variation of SSA tells detailed information about the dominant aerosol types (*e.g.*, black carbon, dust, and sulfate) and can be used in aerosol type identification together with AE or fine-mode fraction (Cheng et al., 2015; Patel et al., 2017).

SSA at four wavelength (440, 675, 870 and 1020 nm) over urban Harbin is retrieved during our study period to further understand local aerosol variations. The seasonal mean spectral variation is presented in Fig. 5. Total mean SSA at 440 nm is 0.93 ± 0.09, showing aerosols over urban Harbin is of slightly absorbing nature. And it is slightly higher than the

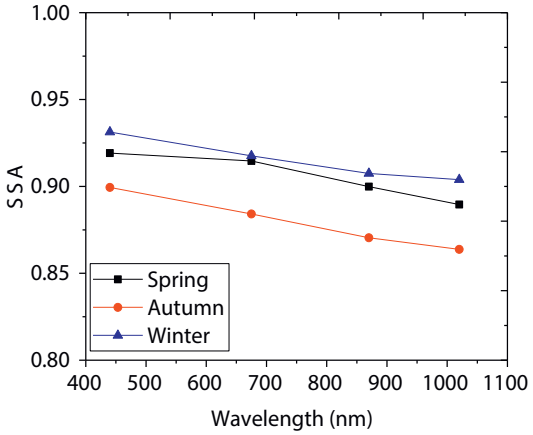

Fig. 5 – Seasonal variation of single scattering albedo over urban Harbin during May 2016 to March 2017.

urban observations in Shanghai (0.91), Xianghe (0.90), and Tongyu (0.91) (Che et al., 2014; Cheng et al., 2015; Zhang et al., 2013). SSA_{440} in the present study region varies a lot and is partly ascribed to the substantial change of aerosol types. Seasonal mean SSA_{440} during spring, autumn, and winter are 0.92 ± 0.04, 0.90 ± 0.12, and 0.93 ± 0.09, respectively. Lower SSA_{440} in autumn is likely due to large amount of strongly absorbing aerosols from crop residue burning and the accumulation of soot particles from coal emission under static and steady weather at the beginning of the heating period (Wang et al., 2016). Higher SSA_{440} in spring is mainly contributed to the influence of long range transport dust. Considering the large amount of precipitation and occasionally high RH in spring, high humidity may enhance the conversion rate of SO_2 to sulfate and promote the photochemistry converting NO_2 to ammonium (Xia et al., 2016; Zhang et al., 2012, 2013), which may also lead to the relative high SSA_{440} in spring.

Spectral variation in SSA differs slightly during different seasons, and this variation lies on the relative proportions of absorbing and scattering components in the atmosphere (Xia et al., 2016). A relatively consistent decrease trend of SSA as the wavelength increases during spring, autumn, and winter indicates the presence of absorbing polluted aerosols. Familiar spectral variation of SSA is found in some regions in China and India during autumn and winter (Patel et al., 2017; Xia et al., 2016).

2.4. ASY

ASY represents the angular distribution of light scattering by atmospheric particles, which plays a key role on controlling aerosol radiative forcing and modifying regional climate (Li et al., 2015; Yu et al., 2009a). ASY is defined as the cosine weighted average of the scattering phase function, and it depends entirely on the physical and chemical properties of aerosol particles, *e.g.*, shape, size and component. The range of ASY varies from −1 to +1, where −1 value represents absolutely backscattered light, 0 value shows a symmetric scattering, and +1 represents entirely forward scattered light (Patel et al., 2017).

Seasonal mean spectral variation of ASY is shown in Fig. 6. ASY during autumn decreases with increase in wavelength, and shows a relatively strong wavelength dependence, indicating the abundance of absorbing polluted aerosols. However, during spring and winter, ASY varies little in the near infrared region, and it can be attributed to the influence of transported coarse mode dust particles. This result is similar to the observation obtained at Beijing, SACOL, Noto, and Shirahama site during the dusty days (Che et al., 2014; Yu et al., 2009b). Seasonal mean ASY_{440} during spring, autumn, and winter are 0.68 ± 0.02, 0.71 ± 0.06, and 0.70 ± 0.05, respectively. Weather condition during autumn and winter over Harbin is characterized of dry and cold with little rainfall and relative low RH (<80%) compared to spring, and the seasonal mean $AE_{440–870}$ values are both larger than 1.0, indicating that the suspended aerosols are mostly fine mode dry aerosol particles. The seasonal mean ASY value during autumn and winter of 0.71 and 0.70 fits well with the conclusions of D'Almeida et al. (1991), who suggested the ASY value of nearly 0.72 represents the fine-mode dry aerosol particles (D'Almeida et al., 1991).

2.5. Discrimination of aerosol types

Aerosol type can be determined by using the information on the spectral variation of optical and physical properties of aerosols. The mostly common and widely used technique for identifying aerosol types is the combined use of AOD and AE, which are associated with the aerosol loading and aerosol size, respectively (Pace et al., 2006; Patel et al., 2017). Fig. 7a shows the scatter plot of the daily mean value of AOD_{440} and $AE_{440–870}$. A wide distribution of $AE_{440–870}$ values for low-to-high AOD_{440} indicates large variability in aerosol properties and it also suggests a mixing state of different aerosol types in the atmosphere over urban Harbin. Before identifying the aerosol types, some threshold values should be taken to quantify the contribution of major aerosol types. More concretely, clean continental aerosols (CC) representing the back conditions over urban Harbin are considered as $AOD_{440} < 0.2$, while long range transported desert dust aerosols (DD) are for $AOD_{440} > 0.4$ and $AE_{440–870} < 0.8$. Cases corresponding to transported biomass burning aerosols or thick urban/industrial plumes (BB/UI) are

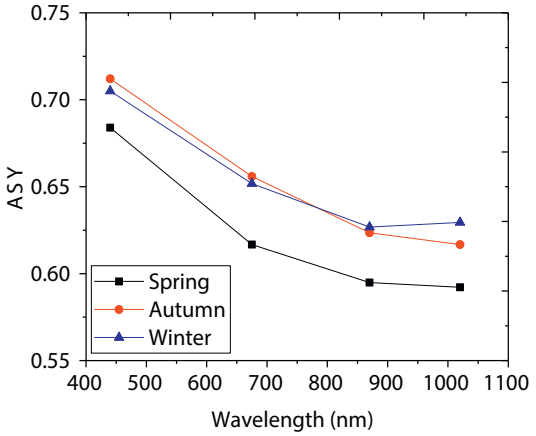

Fig. 6 – Seasonal spectral variation of asymmetry factor over urban Harbin during May 2016 to March 2017.

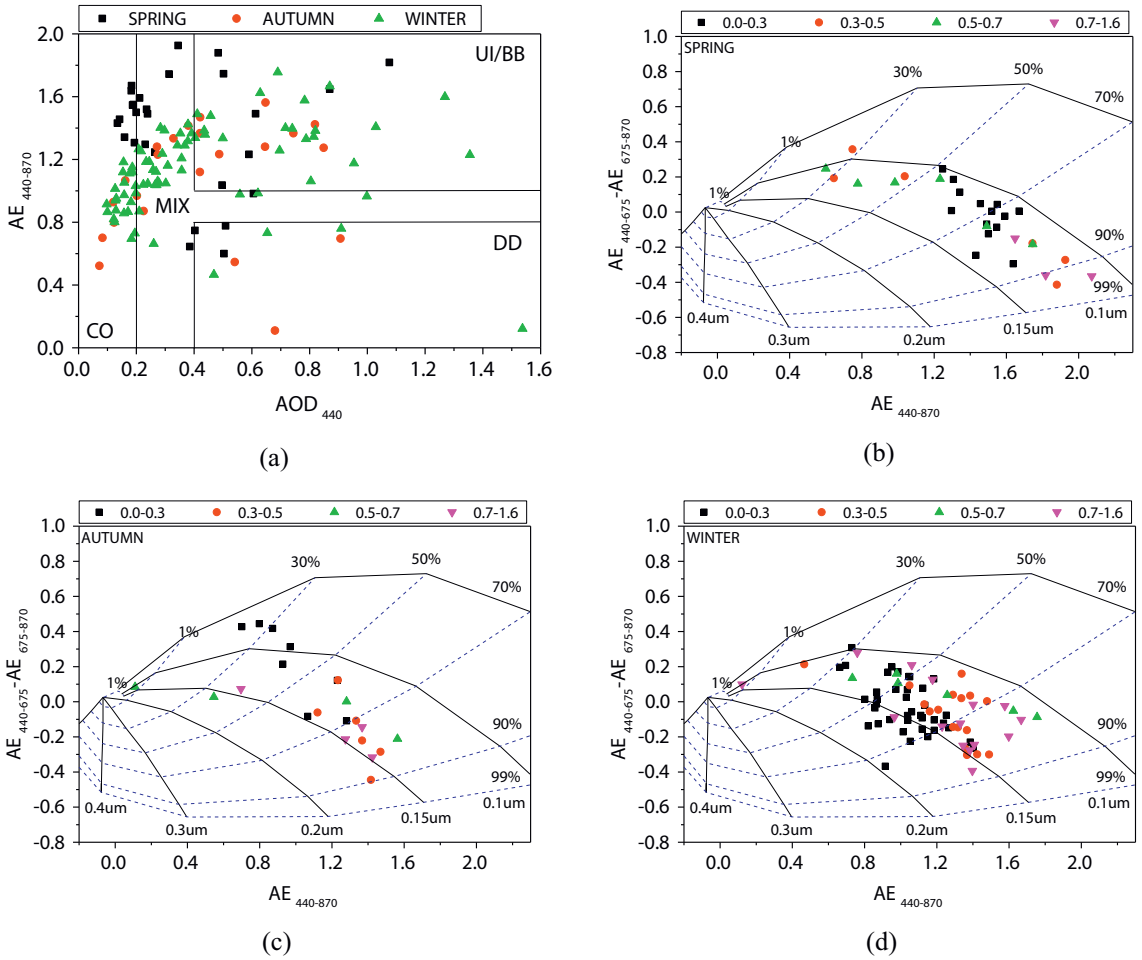

Fig. 7 – (a) Scatter plot of AOD_{440} versus $AE_{440–870}$ with daily average data identifying dominant aerosol types over Harbin during the study period. (b–d) Seasonal mean Ångström exponent difference as a function of $AE_{440–870}$ to and AOD440 (color scale) over Harbin for spring, autumn, and winter respectively. The black lines indicate the fixed fine mode radius and the blue lines the fixed fine mode fraction. AOD: aerosol optical depth; AE: angstrom exponent.

for $AOD_{440} > 0.4$ and $AE_{440–870} > 1.0$, while cases that do not belong to any of the above categories are regarded as mixed type aerosols (MIX). Table 2 gives the total and seasonal contribution of these four aerosol types over Harbin during our studying period. The dominant aerosol type over Harbin is found to be the MIX (34%) with maximum in winter (36%), while BB/UI is found to be the second most contributor (31%). The high contribution of both MIX and BB/UI aerosols suggests that Harbin is strongly affected by a large number of anthropogenic aerosols due to local and transported pollutants (*e.g.*, the agricultural crop-residue burning, automobile exhaust, soot particles of heating). DD aerosols also account for a considerable proportion with relative high percentage in spring (10%) and autumn (13%), rendering Harbin sometimes suffers moderate dust aerosols. It is observed that CC aerosols account for a considerable proportion (27%), indicating that the air quality over Harbin (low aerosol load with $AOD_{440} < 0.2$) is much better than that of most cities in south China (Xia et al., 2016). The results above mostly depend on the threshold set and it may be strongly modifying the contribution when the threshold value changes (Patel et al., 2017).

Table 2 – Percentage of contribution of different aerosol type to the total.

Season	CC	MIX	DD	BB/UI
Spring	28%	34%	10%	26%
Autumn	22%	26%	13%	39%
Winter	29%	36%	5%	30%
Total	27%	34%	8%	31%

CC: continental aerosol; MIX: mixed type aerosol; DD: desert dust aerosol; BB/UI: biomass burning/urban industry aerosol.

A simple graphical method proposed by Gobbi et al. (2007) (Gobbi et al., 2007) is used in the present study to distinguish aerosol growth from cloud contamination and to classify aerosol properties based on the measurements of sun photometer over urban Harbin. The two variables used by this graphical scheme are AE_{440} and the difference of AE (ΔAE) in two individual spectral bands, where the fine mode radii and fine mode fraction (FMF) are used as grid parameters. A large variation is observed during spring, autumn and winter (Fig. 7b–d), indicating significant variation in the dominant particle sizes (Patel et al., 2017). Negative difference of AE suggests the dominance of fine mode particles, while positive value relates to larger fraction of

coarse mode particles under a bimodal size distribution (Zhu et al., 2016). A high value of AOD_{440} (>0.7) occurred during spring relates to fine mode aerosols with FMF > 90% and ΔAE < −0.4, indicating the vast presence of anthropogenic aerosols, while a low value of AOD_{440} (<0.3) is observed with FMF ranging from 50% to 90% and ΔAE from −0.4 to 0.4, rendering the roughly equal presence of both fine and coarse mode aerosols. Cases with moderate AOD_{440} (0.3–0.7) are more inclined to small FMF (<50%) and positive ΔAE values, which suggest the influence of long range transported dust aerosols from west. Same variations of AE_{440} and ΔAE could be found during autumn and winter. In general, the increase of AOD_{440} during autumn and winter is associated with the extension of fine mode radii and FMF, and this pattern is partly similar to that of Beijing, Shanghai, and Nanjing (Cheng et al., 2015; Yu et al., 2016). The hygroscopic or the coagulation growth of aging fine particles may lead to the increase of aerosol load. Overall, the fine mode aerosol size is generally in the range of 0.1 μm to 0.15 μm, and the huge variation of FMF depicts that fine mode particles (mainly corresponding to anthropogenic emissions) is of the most dominance.

3. Conclusions

The data from nine-month ground-based observation conducted over urban Harbin during May 2016 to March 2017 were utilized, for the first time, to analyze regional aerosol optical properties, including AOD, AE, SSA, ASY, and VSD, and the variation of aerosol types.

During our studying period, mean AOD_{440}, $AE_{440–870}$, and WV (in cm) were 0.42 ± 0.29, 1.18 ± 0.34, and 0.97 ± 0.79 cm, respectively, and the large variability in both AOD_{440} and $AE_{440–870}$ indicates the frequent change of aerosol types over urban Harbin. Total mean SSA at 440 nm is 0.93 ± 0.09, showing aerosols over urban Harbin is of slightly absorbing nature, and it is a little higher than the urban observations in Shanghai, Xianghe, and Tongyu. Seasonal mean ASY_{440} during spring, autumn, and winter are 0.68 ± 0.02, 0.71 ± 0.06, and 0.70 ± 0.05, respectively. It is observed that ASY during autumn decreases with increase in wavelength, while it varies little in the near infrared region during winter, indicating the influence of transported coarse mode dust particles. Aerosol volume size distribution was found to be bimodal logarithm distribution with a fine mode radius value of ~ 0.2 μm and coarse mode radius of 3.0–8.0 μm, suggesting the relative equal influence of both fine and coarse model aerosols over Harbin during the whole studying period. Results from aerosol type discrimination indicated the dominance of MIX aerosol and also BB/UI aerosol, while CC aerosols accounted for a considerable proportion (27%), and it means a higher air quality at Harbin than that at most of megacities in south China. And this study will help to improve our understanding of local aerosol properties, regional transport, and their climatic effects over Northeast China Plain.

Acknowledgments

This work was supported by the National Natural Science Foundation of China (Nos. 51776051 and 51406041). A very special acknowledgement is made to the editors and referees who made valuable comments to improve this paper.

Appendix A. Supplementary data

Supplementary data to this article can be found online at https://doi.org/10.1016/j.jes.2018.02.003.

REFERENCES

Bai, Y., Wu, L.X., Qin, K., Zhang, Y.F., Shen, Y.Y., Zhou, Y., 2016. A Geographically and temporally weighted regression model for ground-Level PM2.5 estimation from satellite-derived 500 m resolution AOD. Remote. Sens. Basel. 8.

Che, H., Xia, X., Zhu, J., Li, Z., Dubovik, O., Holben, B., et al., 2014. Column aerosol optical properties and aerosol radiative forcing during a serious haze-fog month over North China Plain in 2013 based on ground-based sunphotometer measurements. Atmos. Chem. Phys. 14, 2125–2138.

Chen, Q.X., Yuan, Y., Huang, X., Jiang, Y.Q., Tan, H.P., 2017. Estimation of surface-level PM2.5 concentration using aerosol optical thickness through aerosol type analysis method. Atmos. Environ. 159, 26–33.

Cheng, T.T., Xu, C., Duan, J.Y., Wang, Y.F., Leng, C.P., Tao, J., et al., 2015. Seasonal variation and difference of aerosol optical properties in columnar and surface atmospheres over Shanghai. Atmos. Environ. 123, 315–326.

D'Almeida, G.A., Koepke, P., Shettle, E.P., 1991. Atmospheric aerosols: global climatology and radiative characteristics. J. Med. Microbiol. 54, 55–61.

Dubovik, O., Smirnov, A., Holben, B.N., King, M.D., Kaufman, Y.J., Eck, T.F., et al., 2000. Accuracy assessments of aerosol optical properties retrieved from Aerosol Robotic Network (AERONET) Sun and sky radiance measurements. J. Geophys. Res. Atmos. 105, 9791–9806.

Dubovik, O., Holben, B., Eck, T.F., Smirnov, A., Kaufman, Y.J., King, M.D., et al., 2002. Variability of absorption and optical properties of key aerosol types observed in worldwide locations. J. Atmos. Sci. 59, 590–608.

Garcia, O.E., Diaz, J.P., Exposito, F.J., Diaz, A.M., Dubovik, O., Derimian, Y., et al., 2012. Shortwave radiative forcing and efficiency of key aerosol types using AERONET data. Atmos. Chem. Phys. 12, 5129–5145.

Gobbi, G.P., Kaufman, Y.J., Koren, I., Eck, T.F., 2007. Classification of aerosol properties derived from AERONET direct sun data. Atmos. Chem. Phys. 7, 453–458.

Haywood, J., Francis, P., Dubovik, O., Glew, M., Holben, B., 2003. Comparison of aerosol size distributions, radiative properties, and optical depths determined by aircraft observations and Sun photometers during SAFARI 2000. J. Geophys. Res. Atmos. 108.

Jiang, M., Sun, W.W., Yang, G., Zhang, D.A.F., 2017. Modelling seasonal GWR of daily PM2.5 with proper auxiliary variables for the Yangtze River Delta. Remote. Sens. Basel. 9.

Kuang, Y., Zhao, C.S., Tao, J.C., Bian, Y.X., Ma, N., 2016. Impact of aerosol hygroscopic growth on the direct aerosol radiative effect in summer on North China Plain. Atmos. Environ. 147, 224–233.

Li, X., Zhang, L., 2012. Analysis of aerosol sources and optical properties based on backward trajectory method over SACOL. Acta. Phys. Sin. Chin. Ed. 61.

Li, Z.Q., Xia, X.G., Cribb, M., Mi, W., Holben, B., Wang, P.C., et al., 2007. Aerosol optical properties and their radiative effects in northern China. J. Geophys. Res. Atmos. 112.

Li, J., Carlson, B.E., Dubovik, O., Lacis, A.A., 2015. Recent trends in aerosol optical properties derived from AERONET measurements. Atmos. Chem. Phys. 15, 1599.
Li, X., Xia, X., Che, H., Yu, X., Liu, Y., Dubovik, O., et al., 2017. Contrast in column-integrated aerosol optical properties during heating and non-heating seasons at Urumqi — its causes and implications. Atmos. Res. 191, 34–43.
Mao, Q.J., 2016. Recent developments in geometrical configurations of thermal energy storage for concentrating solar power plant. Renew. Sust. Energ. Rev. 59, 320–327.
Pace, G., di Sarra, A., Meloni, D., Piacentino, S., Chamard, P., 2006. Aerosol optical properties at Lampedusa (Central Mediterranean). 1. Influence of transport and identification of different aerosol types. Atmos. Chem. Phys. 6, 697–713.
Patel, P.N., Dumka, U.C., Babu, K.N., Mathur, A.K., 2017. Aerosol characterization and radiative properties over Kavaratti, a remote island in southern Arabian Sea from the period of observations. Sci. Total Environ. 599, 165–180.
Russell, P.B., Livingston, J.M., Dubovik, O., Ramirez, S.A., Wang, J., Redemann, J., et al., 2004. Sunlight transmission through desert dust and marine aerosols: diffuse light corrections to Sun photometry and pyrheliometry. J. Geophys. Res. Atmos. 109.
Shi, G.Y., 2007. Atmospheric Radiology. Science Press, Beijing.
Smirnov, A., Holben, B.N., Eck, T.F., Dubovik, O., Slutsker, I., 2003. Effect of wind speed on columnar aerosol optical properties at Midway Island. J. Geophys. Res. Atmos. 108.
Takemura, T., Nakajima, T., Dubovik, O., Holben, B.N., Kinne, S., 2002. Single-scattering albedo and radiative forcing of various aerosol species with a global three-dimensional model. J. Clim. 15, 333–352.
Tanre, D., Kaufman, Y.J., Holben, B.N., Chatenet, B., Karnieli, A., Lavenu, F., et al., 2001. Climatology of dust aerosol size distribution and optical properties derived from remotely sensed data in the solar spectrum. J. Geophys. Res. Atmos. 106, 18205–18217.
Wang, W.Z., Wang, Y.M., Song, W.J., Shi, G.Q., 2016. Evaluation of infrared heat loss of dust-polluted surface atmosphere for solar energy utilization in mine area. Int. J. Hydrogen Energy 41, 15892–15898.
Wang, Y.M., Shi, G.Q., Guo, Z.X., 2017. Heat transfer and thermodynamic processes in coal-bearing strata under the spontaneous combustion condition. Numer. Heat Transf. A Appl. 71, 1–16.
Xia, X., Chen, H., Goloub, P., Zhang, W., Chatenet, B., Wang, P., 2007. A compilation of aerosol optical properties and calculation of direct radiative forcing over an urban region in northern China. J. Geophys. Res. Atmos. 112.
Xia, X.G., Chen, H.B., Goloub, P., Zong, X.M., Zhang, W.X., Wang, P.C., 2013. Climatological aspects of aerosol optical properties in North China Plain based on ground and satellite remote-sensing data. J. Quant. Spectrosc. Radiat. Transf. 127, 12–23.
Xia, X., Che, H., Zhu, J., Chen, H., Cong, Z., Deng, X., et al., 2016. Ground-based remote sensing of aerosol climatology in China: aerosol optical properties, direct radiative effect and its parameterization. Atmos. Environ. 124, 243–251.
Xin, J.Y., Wang, Y.S., Li, Z.Q., Wang, P.C., Hao, W.M., Nordgren, B.L., et al., 2007. Aerosol optical depth (AOD) and Angstrom exponent of aerosols observed by the Chinese Sun Hazemeter Network from August 2004 to September 2005. J. Geophys. Res. Atmos. 112.
Yu, X.N., Zhu, B., Fan, S.X., Yin, Y., Bu, X.L., 2009a. Ground-based observation of aerosol optical properties in Lanzhou, China. J. Environ. Sci. 21, 1519–1524.
Yu, X.N., Zhu, B., Zhang, M.G., 2009b. Seasonal variability of aerosol optical properties over Beijing. Atmos. Environ. 43, 4095–4101.
Yu, X.N., Kumar, K.R., Lu, R., Ma, J., 2016. Changes in column aerosol optical properties during extreme haze-fog episodes in January 2013 over urban Beijing. Environ. Pollut. 210, 217–226.
Zhang, X.L., Mao, M., 2015. Brown haze types due to aerosol pollution at Hefei in the summer and fall. Chemosphere 119, 1153–1162.
Zhang, X.Y., Wang, Y.Q., Niu, T., Zhang, X.C., Gong, S.L., Zhang, Y. M., et al., 2012. Atmospheric aerosol compositions in China: spatial/temporal variability, chemical signature, regional haze distribution and comparisons with global aerosols. Atmos. Chem. Phys. 12, 779–799.
Zhang, Y.S., Shao, M., Lin, Y., Luan, S.J., Mao, N., Chen, W.T., Wang, M., 2013. Emission inventory of carbonaceous pollutants from biomass burning in the Pearl River Delta Region, China. Atmos. Environ. 76, 189–199.
Zhang, Y.J., Sun, Y.L., Du, W., Wang, Q.Q., Chen, C., Han, T.T., et al., 2016. Response of aerosol composition to different emission scenarios in Beijing, China. Sci. Total Environ. 571, 902–908.
Zhu, J., Che, H.Z., Xia, X.G., Chen, H.B., Goloub, P., Zhang, W.X., 2014. Column-integrated aerosol optical and physical properties at a regional background atmosphere in North China Plain. Atmos. Environ. 84, 54–64.
Zhu, J., Xia, X., Che, H., Wang, J., Zhang, J., Duan, Y., 2016. Study of aerosol optical properties at Kunming in southwest China and long-range transport of biomass burning aerosols from North Burma. Atmos. Res. 169, 237–247.
Zou, B., Chen, J.W., Zhai, L., Fang, X., Zheng, Z., 2017. Satellite based mapping of ground PM2.5 concentration using generalized additive modeling. Remote. Sens. Basel 9.